

Synthesis of Cage Compounds Containing Boron, Germanium, and Phosphorus Atoms

Tuqiang Chen,[†] Eileen N. Duesler,[†] Robert T. Paine,^{*,†} and H. Nöth^{*,†}

Department of Chemistry, University of New Mexico, Albuquerque, New Mexico 87131, and Institut für Anorganische Chemie, Universität München, 80333 München, Germany

Received August 22, 1996[⊗]

The 1:1 reactions of [$(i\text{Pr}_2\text{N})\text{BP}(\text{H})\text{B}(\text{N}^i\text{Pr}_2)\text{PLi}\cdot\text{DME}$] and [$(\text{tmp})\text{BP}(\text{H})\text{B}(\text{tmp})\text{PLi}\cdot\text{DME}$] ($\text{tmp} = 2,2,6,6$ -tetramethylpiperidino) with organylhalogermanes have been surveyed, and germyl-substituted diphosphadiboretanes of the type $\text{R}_2\text{NBP}(\text{H})\text{B}(\text{NR}_2)\text{PGe}(\text{Cl})\text{R}'_2$ ($\text{R}_2\text{N} = i\text{Pr}_2\text{N}$, tmp ; $\text{Ge}(\text{Cl})\text{R}'_2 = \text{Ge}(\text{Cl})\text{Me}_2$ and $\text{Ge}(\text{Cl})\text{Ph}_2$) have been isolated and characterized. Subsequent dehydrohalogenation of these compounds with $t\text{BuLi}$ gave the new bicyclic cage compounds $\text{P}_2(\text{BNR}_2)_2(\text{GeR}'_2)$ ($\text{R}_2\text{N} = \text{tmp}$, $\text{R}' = \text{Ph}$; $\text{R}_2\text{N} = \text{tmp}$, $\text{R}' = \text{Me}$) and/or oligomers [$-(\text{R}_2\text{N})\text{BP}(\text{H})\text{B}(\text{NR}_2)\text{PGeR}'_2-$] $_n$ ($\text{R}_2\text{N} = i\text{Pr}_2\text{N}$, $\text{R}' = \text{Me}$; $\text{R}_2\text{N} = \text{tmp}$, $\text{R}' = \text{Me}$). In addition, the 2:1 reactions of [$(\text{R}_2\text{N})\text{BP}(\text{H})\text{B}(\text{NR}_2)\text{PLi}\cdot\text{DME}$] with $\text{R}'_2\text{GeCl}_2$ have been examined. In one case, the cage compound $\text{P}_2(\text{BNR}_2)_2\text{GeR}'_2$ ($\text{R}_2\text{N} = \text{tmp}$, $\text{R}' = \text{Ph}$) was obtained while a smaller alkyl group on Ge allowed formation of the bis(diphosphadiboretanyl)germanes [$\text{R}_2\text{NBP}(\text{H})\text{B}(\text{NR}_2)\text{P}$] $_2\text{GeR}'_2$ ($\text{R}_2\text{N} = i\text{Pr}_2\text{N}$, tmp ; $\text{R}' = \text{Me}$). Two $\text{P}_2(\text{BNR}_2)_2(\text{GeR}'_2)\cdot\text{Cr}(\text{CO})_5$ (complexes $\text{R}_2\text{N} = \text{tmp}$, $\text{R}' = \text{Ph}$, Me) were isolated and characterized. The molecular structures of the cage compound $\text{P}_2(\text{Btmp})_2\text{GePh}_2$ and the complexes $\text{P}_2(\text{Btmp})_2\text{GeR}'_2\cdot\text{Cr}(\text{CO})_5$ ($\text{R}' = \text{Ph}$, Me) were determined with single-crystal X-ray diffraction techniques. The structural and spectroscopic features are discussed in relation to those of other $\text{P}_2(\text{BNR}_2)_2(\text{ER}_2)$ species.

1. Introduction

Main group element cage compounds continue to attract attention due to their fundamentally interesting structural and electronic features,^{1,2} as well as their potential utility as solid state materials precursors. However, in order to find use in practical applications, systematic preparative approaches for the required building blocks must be developed. For example, phosphinoborane ring compounds should provide useful starting materials for the systematic construction of B_xP_y cage species if appropriate substitution and elimination chemistry can be developed, and these species may serve as precursors to solid state boron phosphides. For example, Nöth and co-workers³ found that boron–phosphorus tetrahedrane analogs $(\text{R}_2\text{NBP})_2$ are obtained in good yield from the photolysis of selected diphosphadiboretane rings, $(\text{R}_2\text{NBPCEt}_3)_2$ ($\text{R}_2\text{N} = \text{tmp}$,⁴ $t\text{Bu}_2\text{N}$), and efforts are still in progress to generalize this approach. Several thermally driven reactions have been examined for formation of boron phosphorus cage species. In particular, thermolysis of a 1:2 mixture of $(i\text{Pr}_2\text{N})\text{BCl}_2$ and $(i\text{Pr}_2\text{N})\text{B}$

$(\text{Cl})\text{P}(\text{SiMe}_3)_2$ gives a trigonal-bipyramidal cage $\text{P}_2(i\text{Pr}_2\text{NB})_3$,⁵ however, this approach was not generally useful with other substituent groups. It was observed that a more useful approach to $\text{P}_2(\text{R}_2\text{NB})_2(\text{E})$ cages ($\text{E} = \text{BNR}_2$) is available through the sequential substitution and elimination chemistry summarized in Scheme 1.⁶ This approach should be relatively general for compounds with a variety of other heteroatoms and heteroatom groups. We recently reported the synthesis and structural characterization of analogs containing E ($\text{E} = \text{SiR}_2$, $\text{R}_2\text{Si}-\text{SiR}_2$),⁷ and we report here the extension of this chemistry to include cages containing GeR_2 groups as constituents.

Experimental Section

General Information. Standard inert-atmosphere techniques were used for the manipulations of all reagents and reaction products. Infrared spectra were recorded on a Matteson 2020 FT-infrared spectrometer from solution cells or from KBr pellets. Mass spectra were obtained from a Finnegan mass spectrometer by using a heated solids inlet probe. NMR spectra were recorded on Bruker WP-250 and JEOL GSX-400 spectrometers. The NMR samples were contained in sealed 5 mm tubes with deuterated lock solvent, and spectra were referenced with Me_4Si (^1H , ^{13}C), 85% H_3PO_4 (^{31}P), and $\text{F}_3\text{B}\cdot\text{OEt}_2$ (^{11}B). Elemental analysis data were determined in the UNM microanalytical services laboratory.

Materials. Reagents $i\text{Pr}_2\text{NBCl}_2$,⁸ $(\text{tmp})\text{BCl}_2$,⁹ $\text{LiPH}_2\cdot\text{DME}$,¹⁰ $(i\text{Pr}_2\text{NBP}(\text{H})(i\text{Pr}_2\text{NB})\text{PLi}\cdot\text{DME})^{7,11}$ (**3**), $(\text{tmp})\text{BP}(\text{H})(\text{tmp})\text{B}\text{PLi}\cdot\text{DME}^{11}$

[†] University of New Mexico.

[‡] Universität München.

[⊗] Abstract published in *Advance ACS Abstracts*, February 1, 1997.

- (1) Grimes, R. N. *Carboranes*; Academic Press: New York, 1970. Beall, H. In *Boron Hydride Chemistry*; Muettterties, E. L., Ed.; Academic Press: New York, 1975; Chapter 9. Onak, T. *Ibid.*; Chapter 10. Dunks, G. B.; Hawthorne, M. F. *Ibid.*; Chapter 11. Callahan, K. P.; Hawthorne, M. F. *Adv. Organomet. Chem.* **1976**, *14*, 145. Grimes, R. N. *Pure Appl. Chem.* **1974**, *39*, 455. Callahan, K. P.; Hawthorne, M. F. *Ibid.* **1974**, *39*, 475.
- (2) Sowerby, D. B. In *The Chemistry of Inorganic Homo- and Heterocycles*; Haiduc, I., Sowerby, D. B., Eds.; Academic Press: New York, 1987.
- (3) Kölle, P.; Linti, G.; Nöth, H.; Polborn, K. *J. Organomet. Chem.* **1988**, *355*, 7.
- (4) Abbreviations used in the text include tmp = 2,2,6,6-tetramethylpiperidino, Me = Methyl, tms = trimethylsilyl, THF = tetrahydrofuran, $i\text{Pr}$ = isopropyl, and DME = ethylene glycol dimethyl ether, and $t\text{Bu}$ = *tert*-butyl.

(5) Wood, G. L.; Duesler, E. N.; Narula, C. K.; Paine, R. T.; Nöth, H. *J. Chem. Soc., Chem. Commun.* **1987**, 496.

(6) Dou, D.; Wood, G. L.; Duesler, E. N.; Paine, R. T.; Nöth, H. *Inorg. Chem.* **1992**, *31*, 3756.

(7) Dou, D.; Kaufmann, B.; Duesler, E. N.; Chen, T.; Paine, R. T.; Nöth, H. *Inorg. Chem.* **1993**, *32*, 3056.

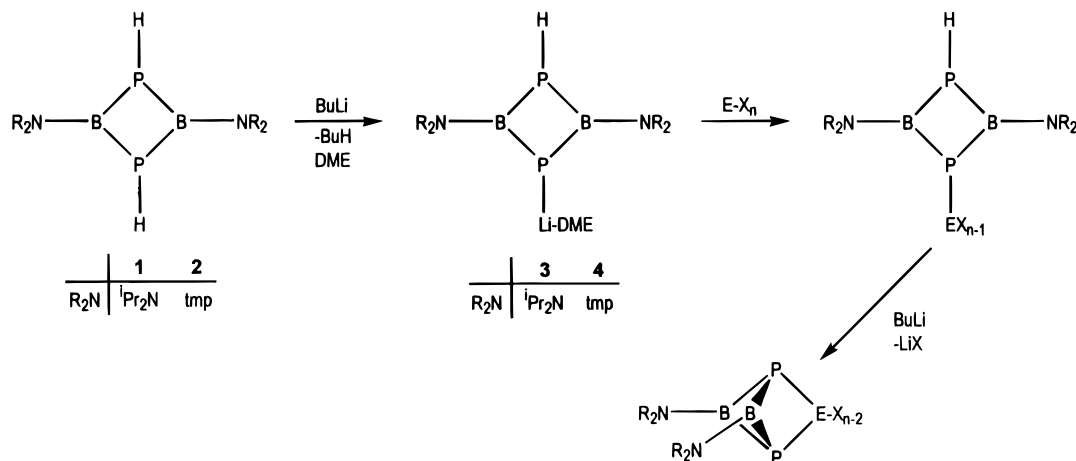
(8) Gerrard, W.; Hudson, H. R.; Mooney, E. R. *J. Chem. Soc.* **1960**, 5168.

(9) Nöth, H.; Weber, S. Z. *Naturforsch., B* **1983**, *37*, 1460.

(10) Schäfer, H.; Fritz, G.; Hölderich, W. Z. *Anorg. Chem.* **1977**, *428*, 222.

(11) Dou, D.; Westerhausen, M.; Wood, G. L.; Linti, G.; Duesler, E. N.; Nöth, H.; Paine, R. T. *Chem. Ber.*, **1993**, *126*, 379.

Scheme 1



(4), and $(\text{CO})_5\text{Cr}\cdot\text{NMe}_3^{12}$ were prepared as described in the literature. The samples of Me_2GeCl_2 and Ph_2GeCl_2 were purchased from Strem Chemical Co., and BuLi solutions were obtained from Aldrich Chemical Co. Solvents were rigorously dried and degassed by standard methods. Solvent transfers were accomplished by vacuum distillation, and all product work-ups were performed in Schlenkware under dry nitrogen.

Synthesis and Characterization of Compounds. 2,4-Bis(dialkyl-amino)-1-(diorganochlorogermyl)-1,3,2,4-diphosphadiboretanes (5, 6, 7, and 8). Each of these compounds was prepared in a related fashion illustrated by the specific synthesis for 5. A sample of

$(\text{Pr}_2\text{N})\text{BP}(\text{H})(\text{Pr}_2\text{NB})\text{PLi}\cdot\text{DME}$ (**3**) (2.11 g, 5.50 mmol) was added with stirring to a cold (-78°C) hexane (40 mL) solution of Me_2GeCl_2 (0.96 g, 5.5 mmol). The cloudy mixture was stirred at -78°C (2 h) and at 23°C (15 h). The resulting mixture was filtered and the filtrate collected. Further work-up details and characterization data are individually described.

Compound **5** was recovered as a yellow oil from the filtrate by vacuum evaporation. After several days at 23°C , the oil fully crystallized as a pale yellow solid and no further purification was required: yield 2.3 g (100%); mp $101\text{--}104^\circ\text{C}$. Mass spectrum (30 eV) [m/e (%): 428–419 (M^+ , 424 most intense, 44%), 389–383 (388 most intense, 10%), 285 (100%)]. Infrared spectrum (KBr, cm^{-1}): 2971 (s), 2928 (s), 2870 (s), 2253 (s), 1465 (s), 1445 (s), 1366 (s), 1312 (s), 1231 (m), 1182 (s), 1142 (s), 1001 (m), 870 (m), 841 (m), 806 (s), 716 (m), 606 (m), 574 (m), 546 (m), 530 (w). Anal. Calcd for $\text{C}_{14}\text{H}_{35}\text{B}_2\text{N}_2\text{P}_2\text{ClGe}$ (423.04): C, 39.75; H, 8.34; N, 6.62. Found: C, 40.18; H, 9.09; N, 6.49.

Compound **6** was not isolated and it was only characterized by ^{31}P NMR spectroscopy.

Compound **7** was obtained as pale yellow crystals by concentrating the final filtrate to a few milliliters and cooling to -10°C : yield 0.90 g, (81%); mp $158\text{--}160^\circ\text{C}$ dec. Mass spectrum (30 eV) [m/e (%): 506–500 (M^+ , 504 most intense, 35%), 469–464 (468 most intense, 28%), 366–363 ($\text{M} - \text{tmp}^+$, 365 most intense, 100%)]. Infrared spectrum (KBr, cm^{-1}): 2963 (s), 2938 (s), 2868 (m), 2249 (m), 1464 (m), 1381 (s), 1369 (s), 1330 (s), 1300 (m), 1300 (m), 1240 (m), 1231 (m), 1190 (w), 1163 (m), 1128 (m), 1088 (w), 1042 (w), 988 (m), 904 (w), 858 (w), 839 (w), 808 (m), 704 (w), 611 (w), 575 (w), 498 (w). Anal. Calcd for $\text{C}_{20}\text{H}_{43}\text{B}_2\text{N}_2\text{P}_2\text{ClGe}$ (503.16): C, 47.74; H, 8.61; N, 5.57. Found: C, 47.64; H, 8.64; N, 5.48.

Compound **8** was isolated by evaporating the hexane suspension, redissolving it in Et_2O (20 mL), filtering, and evaporating the Et_2O from the filtrate. The resulting pale yellow powder was washed with cold hexane and the product recovered as a colorless powder: yield 1.70 g (85.0%); mp $55\text{--}57^\circ\text{C}$. Mass spectrum (30 eV) [m/e (%): 366–363 ($\text{M} - \text{Ph}_2\text{GeCl}^+$, 365 most intense, 14%), 333 (4%)]. Infrared spectrum (KBr, cm^{-1}): 3052 (w), 2967 (s), 2934 (s), 2870 (m), 2240 (m), 1464 (m), 1431 (m), 1370 (vs), 1333 (s), 1302 (m), 1240 (w), 1165 (m), 1127 (m), 1084 (w), 1044 (w), 988 (m), 862 (w), 816 (w),

733 (m), 696 (m), 575 (w), 472 (m). Anal. Calcd for $\text{C}_{30}\text{H}_{47}\text{B}_2\text{N}_2\text{P}_2\text{ClGe}$ (627.30): C, 57.44; H, 7.55; N, 4.47. Found: C, 57.91; H, 7.81; N, 4.41.

2,4-Bis(2,2,6,6-tetramethylpiperidino)-5-dimethyl-1,3-diphosphadibora-5-germabicyclo[1.1.1]pentane (9). A solution containing **7** (1.40 g, 2.8 mmol) in hexane (30 mL) was cooled to -78°C , and BuLi (1.6 mL, 2.7 mmol, 1.7 M in pentane) solution was dripped into the stirred solution through an airtight syringe. The resulting cloudy yellow mixture was stirred at -78°C (2 h), slowly warmed to 23°C , and stirred (16 h), and then filtered and the solvent removed from the filtrate. A yellow crystalline solid and yellow oil remained. This mixture was crystallized from cold hexane (-10°C , ~ 5 mL) providing pale yellow crystals: yield 0.25 g (19%); mp $101\text{--}104^\circ\text{C}$ dec. Mass spectrum (30 eV) [m/e (%): 471–463 (M^+ , 467 most intense, 47%)]. Anal. Calcd for $\text{C}_{20}\text{H}_{42}\text{B}_2\text{N}_2\text{P}_2\text{Ge}$ (466.71): C, 51.47; H, 9.07; N, 6.00. Found: C, 51.11; H, 10.17; N, 5.88.

2,4-Bis(2,2,6,6-tetramethylpiperidino)-5-diphenyl-1,3-diphosphadibora-5-germabicyclo[1.1.1]pentane (10). A suspension of **8** (0.95 g, 1.5 mmol) in hexane (30 mL) was cooled to -78°C and a BuLi (0.90 mL, 1.5 mmol, 1.7 M in pentane) solution was dripped into the stirred suspension through an airtight syringe. The resulting yellow reaction mixture was warmed slowly (2 h) to 23°C and stirred (15 h). The suspension was then filtered and the solvent removed from the filtrate by vacuum evaporation. The yellow residue was recrystallized from cold hexane (-10°C , 10 mL). Pale yellow crystals were obtained: yield 0.39 g (44%); mp $196\text{--}198^\circ\text{C}$. Mass spectrum (30 eV) [m/e (%): 596–587 (M^+ , 592 most intense, 100%)]. Infrared spectrum (KBr, cm^{-1}): 3061 (w), 2961 (s), 2936 (s), 2864 (m), 1582 (w), 1465 (m), 1431 (m), 1364 (s), 1331 (s), 1287 (m), 1252 (m), 1171 (m), 1128 (m), 1086 (w), 993 (m), 976 (m), 735 (s), 698 (m), 571 (w), 471 (m). Anal. Calcd for $\text{C}_{30}\text{H}_{46}\text{B}_2\text{N}_2\text{P}_2\text{Ge}$ (590.84): C, 60.98; H, 7.85; N, 4.74. Found: C, 61.11; H, 7.97; N, 4.84.

Dimethylbis[2,4-bis(diisopropylamino)-1,3,2,4-diphosphadiboretanyl]germane (11). A solid sample of **3** (1.40 g, 3.6 mmol) was added to a cold (-78°C) hexane solution (40 mL) containing Me_2GeCl_2 (0.30 g, 1.7 mmol). The mixture was stirred at -78°C (2 h) and then at 23°C (15 h) and then filtered. The filtrate was vacuum evaporated leaving a pale yellow oil which solidified on standing at 23°C for several days. No further purification was required. Yield: 1.20 g (100%). Mp: $114\text{--}118^\circ\text{C}$. Mass spectrum (30 eV) [m/e (%): 386 (87%), 285 (9%)]. Infrared spectrum (KBr, cm^{-1}): 2967 (s), 2928 (s), 2868 (m), 2247 (m), 2232 (m), 2221 (m), 1468 (s), 1443 (s), 1366 (s), 1310 (s), 1221 (w), 1184 (m), 1145 (s), 1005 (m), 872 (w), 829 (w), 783 (m), 723 (w), 577 (m), 542 (w). Anal. Calcd for $\text{C}_{26}\text{H}_{62}\text{B}_2\text{N}_2\text{P}_2\text{Ge}$ (670.51): C, 46.57; H, 9.32; N, 8.36. Found: C, 47.04; H, 9.67; N, 8.44.

Dimethylbis[2,4-bis(2,2,6,6-tetramethylpiperidino)-1,3,2,4-diphosphadiboretanyl]germane (12). A solid sample of $(\text{tmp})\text{BP}(\text{H})\cdot(\text{tmp})\text{BPLi}\cdot\text{DME}$, **4** (1.07 g, 2.3 mmol), was added to a cold (-78°C) hexane solution (40 mL) containing Me_2GeCl_2 (0.20 g, 1.2 mmol). The mixture was stirred at -78°C (2 h) and then at 23°C (15 h) and then filtered. The filtrate was vacuum evaporated, leaving a pale yellow

(12) Wasserman, H. J.; Workulich, M. J.; Atwood, J. D.; Churchill, M. R. *Inorg. Chem.* **1980**, *19*, 2831.

Table 1. Crystallographic Data for P₂(tmpB)₂(GePh₂) (**10**), P₂(tmpB)₂(GePh₂)·Cr(CO)₅ (**13**) and P₂(tmpB)₂(GeMe₂)·Cr(CO)₅ (**14**)

	10	13	14
chem formula	C ₃₀ H ₄₆ B ₂ N ₂ GeP ₂	C ₃₅ H ₄₆ B ₂ N ₂ O ₅ GeP ₂ Cr	C ₂₅ H ₄₂ B ₂ N ₂ O ₅ P ₂ GeCr
<i>a</i> , Å	8.586(2)	12.040(2)	14.969(1)
<i>b</i> , Å	16.809(3)	19.862(4)	12.011(1)
<i>c</i> , Å	22.240(4)	16.680(3)	18.185(2)
α, deg	90	90	90
β, deg	90	104.06(3)	97.95(1)
γ, deg	90	90	90
<i>V</i> , Å ³	3209.7(11)	3869.4(12)	3237.9(5)
<i>Z</i>	4	4	4
ρ _{calcd} , g cm ⁻³	1.223	1.344	1.397
fw	590.8	782.9	658.8
cryst dimens, mm	0.25 × 0.25 × 0.92	0.21 × 0.58 × 0.69	0.23 × 0.46 × 0.67
cryst syst	orthorhombic	monoclinic	monoclinic
space group	<i>P</i> 2 ₁ 2 ₁ 2 ₁	<i>P</i> 2 ₁ / <i>c</i>	<i>P</i> 2 ₁ / <i>c</i>
<i>T</i> , °C	20	20	20
μ, cm ⁻¹	10.75	11.81	13.97
2θ range, deg	3–50	3–47	2–52
no. of reflns measd	± <i>h</i> , ± <i>k</i> , ± <i>l</i>	± <i>h</i> , ± <i>k</i> , ± <i>l</i>	± <i>h</i> , ± <i>k</i> , ± <i>l</i>
no. of colld reflns	6464	11 367	13 488
no. of unique reflns	5651	5689	6360
no. of obsd reflns	3434 (<i>F</i> > 2σ(<i>F</i>))	5231 (<i>F</i> > 1.4σ(<i>F</i>))	3534 (<i>F</i> > 2σ(<i>F</i>))
trans coeff (min/max)	0.8069/0.8957	0.6664/1.0000	0.7398/1.0000
<i>R</i> _F , <i>R</i> _{wF} ^a	0.0625, 0.0600	0.0540, 0.0248	0.0424, 0.0332
<i>g</i>	0.0007	0.00001	0.0001

$$^a R = \sum(|F_o| - |F_c|) / \sum|F_o|, R_{wF} = [\sum w(|F_o| - |F_c|)^2 / \sum w F_o^2], w^{-1} = \sigma^2(F) + gF^2.$$

powder that was recrystallized from cold hexane (−10 °C, ~5 mL): yield 0.75 g (78%). The product was contaminated with less than 5% of **8**, ((tmp)BP)₂, and ((tmp)BP)₂ as indicated by characteristic ³¹P NMR resonances. Due to these small impurities, the samples did not provide satisfactory elemental analyses. Infrared spectrum (KBr, cm⁻¹):

2965 (s), 2932 (s), 2868 (s), 2268 (m), 2224 (s), 1464 (m), 1369 (s), 1361 (s), 1325 (s), 1300 (s), 1242 (w), 1229 (w), 1194 (w), 1169 (s), 1128 (m), 1090 (w), 1067 (w), 1044 (w), 990 (m), 907 (m), 862 (w), 797 (m), 746 (w), 700 (w), 573 (w).

(2,4-Bis(2,2,6,6-tetramethylpiperidino)-5-diphenyl-1,3-diphospha-2,4-dibora-5-germabicyclo[1.1.1]pentane)chromium Pentacarbonyl (13). Equimolar amounts (1.0 mmol) of Cr(CO)₅·NMe₃ and **10** were combined in 50 mL of hexane at 23 °C, stirred (7 d), and filtered. The filtrate was concentrated (15 mL) and cooled (−10 °C) and yellow crystals deposited: yield 0.45 g (57%); mp 89–91 °C dec. Mass spectrum (30 eV) [*m/e* (%): 784–781 (M⁺, 2%), 591 (M – Cr(CO)₅⁺; 8%). Infrared spectrum (KBr, cm⁻¹): 3065 (w), 2965 (m), 2938 (m), 2054 (m), 1985 (m), 1921 (s), 1466 (w), 1431 (w), 1373 (m), 1343 (m), 1285 (w), 1251 (w), 1171 (w), 1127 (w), 1084 (w), 970 (w), 733 (w), 696 (w), 654 (m), 555 (w), 461 (m). Anal. Calcd for C₃₅H₄₆B₂N₂P₂Ge (782.85): C, 53.69; H, 5.94; N, 3.58. Found: C, 53.67; H, 5.80; N, 3.62.

(2,4-Bis(2,2,6,6-tetramethylpiperidino)-5-dimethyl-1,3-diphospha-2,4-dibora-5-germabicyclo[1.1.1]pentane)chromium Pentacarbonyl (14). Equimolar amounts (1.0 mmol) of Cr(CO)₅·NMe₃ and **7** were combined in 30 mL of hexane at 23 °C. The yellow mixture was stirred (3 d) and then filtered to remove the white solid that formed [Me₃NH]Cl. The filtrate was concentrated to 10 mL and cooled (−10 °C). Yellow crystals of **14** deposited and were collected by filtration: yield 0.25 g (38%); mp 158–160 °C dec. Infrared spectrum (KBr, cm⁻¹): 2963 (w), 2051 (m), 1989 (w), 1925 (s), 1910 (s), 1466 (w), 1366 (w), 1337 (w), 1292 (w), 1252 (w), 1227 (w), 1169 (w), 1127 (w), 988 (m), 669 (m), 656 (m), 425 (w). Anal. Calcd for C₂₉H₄₂B₂N₂O₅P₂GeCr: C, 45.58; H, 6.43; N, 4.25. Found: C, 45.21; H, 6.64; N, 4.27.

Reaction of 5 with ^tBuLi. A solution of **5** (1.49 g, 3.0 mmol) in hexane (30 mL) was cooled (−78 °C) and ^tBuLi (1.7 mL, 2.9 mmol, 1.7 M in pentane) was added through an airtight syringe. The pale yellow suspension was stirred at −78 °C (2 h) and then at 23 °C (16 h). The resulting mixture was filtered and the filtrate evaporated, and 1.36 g of a glassy pale yellow solid **15** was obtained. Cryoscopic molecular weight analysis in benzene gave MW(av) = 1180 (*n* = 4.6).

Crystallographic Measurements and Structure Solutions. Crystals of **10**, **13**, and **14** were placed in glass capillaries under a dry nitrogen atmosphere. The crystals were centered on a Syntex P3/F automated diffractometer and determinations of crystal class, orientation

matrix and unit cell dimensions were performed in a standard manner. Selected crystallographic data are summarized in Table 1. Data were collected in the ω scan mode with Mo Kα (λ = 0.710 73 Å) radiation, a scintillation counter, and a pulse height analyzer. In all cases inspection of a small data set led to assignment of the space groups.¹³ Empirical adsorption corrections were applied, based on ψ scans.¹⁴ No signs of crystal decay were noted for **10** and **13**; however, **14** displayed a 6.5% decline in standard intensities, and the intensity data were scaled accordingly.

All calculations were performed on a Siemens SHELXTL PLUS structure determination system.¹⁵ Solutions for the data sets were by direct methods (**10** and **13**) and by heavy atom methods (**14**), and full-matrix refinements were employed.¹⁶ Neutral atom scattering factors and anomalous dispersion terms were used for all non-hydrogen atoms during the refinements. The function minimized was Σw(|F_o| – |F_c|)². Refinements for **10** and **13** gave no unusual features. Compound **14**, however, showed large thermal motions in the tmp group containing N(2). Disorder models were evaluated, but only one discrete peak per C atom was found. The second tmp group is well behaved. In each molecule the nonhydrogen atoms were refined anisotropically and H atoms were placed in idealized positions (riding model) with *U*_{iso} = 1.25*U*_{equiv}.

Results and Discussion

The generality of the chemistry summarized in Scheme 1 has been further tested by exploring the reactions of the lithium salts ^tPr₂NBP(H)(^tPr₂NB)PLi·DME^{7,11} **3** and (tmp)BP(H)-((tmp)B)PLi·DME¹¹ **4** with Me₂GeCl₂ and Ph₂GeCl₂ as summarized in eq 1. The P-germylated diphosphadiboretanes **5**, **7**,

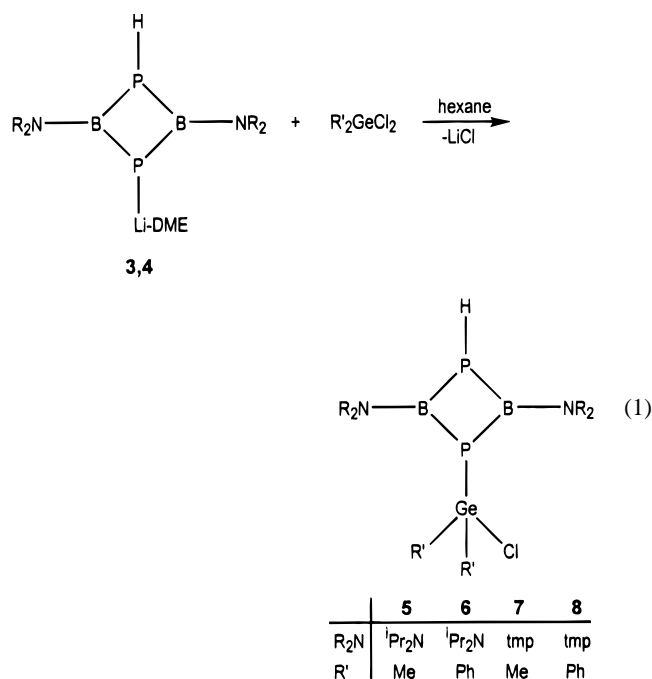
(13) Space group notation is given in: *International Tables for X-Ray Crystallography*; Reidel: Dordrecht, The Netherlands, 1983; Vol. I, pp 73–346.

(14) The empirical absorption corrections use an ellipsoidal model fitted to azimuthal scan data that are then applied to the intensity data: *SHELXTL Manual, Revision 4*; Nicolet XRD Corp.: Madison, WI, 1983.

(15) Sheldrick, G. M. *Nicolet SHELXTL Operations Manual*; Nicolet XRD Corp.: Cupertino, CA, 1981. SHELXTL uses absorption, anomalous dispersion, and scattering data compiled in *International Tables for X-Ray Crystallography*; Knyoch: Birmingham, England, 1974; Vol. IV, pp 55–60, 99–101, 149–150. Anomalous dispersion terms were included for all atoms with atomic numbers greater than 2.

(16) A general description of the least-squares algebra is found in *Crystallographic Computing*; Ahmed, F. R., Hall, S. R., Huber, C. P., Eds.; Munksgaard: Copenhagen, 1970; p 187. The least-squares refinement minimizes Σw(|F_o| – |F_c|)².

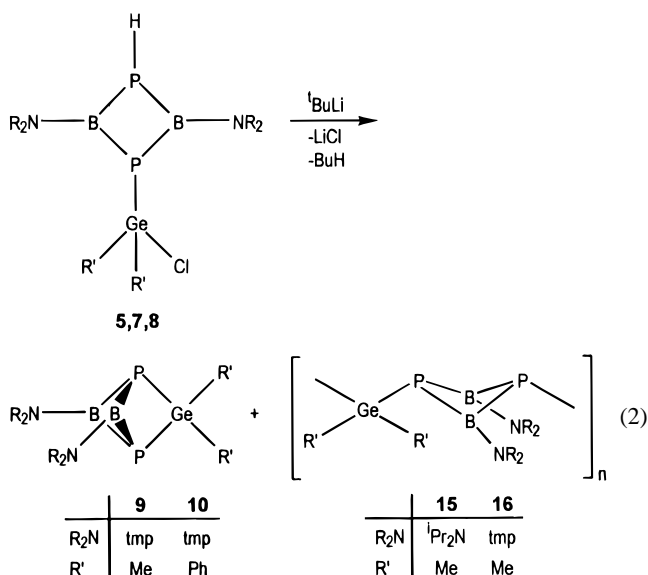
and **8** are isolated in high yields as crystalline solids, and they have been fully characterized. Compound **6** is obtained as a viscous oil that could not be purified, and it is characterized here only by ^{31}P NMR spectroscopy. Compounds **5**, **7**, and **8** give satisfactory elemental analyses, and **5** and **7** display a strong parent ion in their electron impact mass spectra. Compound **8**, however, does not display a parent ion under the conditions employed, and the highest mass ion corresponds to $[\text{M} - (\text{GeClPh}_2)^+]$. It is interesting that, of the P-silylated 1,3,2,4-diphosphadiboretanes reported previously,⁷ only the closely related compound $(\text{tmp})\text{BP}(\text{H})\text{B}(\text{tmp})\text{PSi}(\text{Cl})\text{Ph}_2$ failed to produce a parent ion, suggesting that the P–E(Cl)Ph₂ bond in these compounds may be particularly weak. Each of **5**, **7**, and **8** shows an infrared band in the region 2253–2240 cm^{-1} that is assigned to the terminal P–H stretching vibration, and these compare favorably with values (2281–2226 cm^{-1}) for related silyl derivatives.¹⁷



The NMR spectra for **5–8** are summarized in Table 2. Each compound displays a single $^{11}\text{B}\{^1\text{H}\}$ NMR resonance in the region δ 49.3–47.1 with the resonance for the (tmp)B derivatives appearing at slightly lower field than the resonance for the $^i\text{Pr}_2\text{NB}$ derivative. A similar trend was observed for the P-silyl derivatives.⁷ The $^{31}\text{P}\{^1\text{H}\}$ NMR spectra of **5–8** reveal two peaks of equal intensity. The peak corresponding to the diborylphosphane fragment B_2PH is easily assigned since it splits into a widely spaced (~ 200 Hz) doublet with restoration of P–H coupling. In the $^i\text{Pr}_2\text{NB}$ derivatives, **5** and **6**, the B_2PH resonance appears at higher field while in the (tmp)B derivatives, **7** and **8**, the B_2PH resonance is the lower field resonance of the pair. It is also found that both ^{31}P resonances in **7** and **8** are split into doublets ($^2J_{\text{PP}} = 48\text{--}52$ Hz) due to the inequivalency of the phosphorus environments in the ring. This coupling is not resolved for **5** and **6**. The ^1H NMR spectra for **5**, **7**, and **8** are easily assigned based upon peak intensities, and they are consistent with the proposed structures. As expected, the ^iPr groups show inequivalent CH and CH_3 environments as a result of hindered rotation about the B–N bond and the asymmetry in the phosphorus substituents. The Me_2Ge resonance in **5** and **7** is split into a single doublet, $^3J_{\text{PH}} = 1.9$ and 0.9 Hz, respectively, by the neighboring phosphorus atom. Coupling to the second, inequivalent phosphorus atom is not resolved.

Full assignment of the ^{13}C NMR spectra through nuclear correlations was not attempted in this study.

Dehydrohalogenation of **5**, **7**, and $\mathbf{8}$ promoted with $^t\text{BuLi}$ was examined, and the results are summarized in eq 2. Compound



5 produces a glassy yellow solid that is soluble in benzene. Cryoscopic molecular weight measurements in benzene give an average value for the molecular weight of 1180 which corresponds to $n = 4.6$. The $^{31}\text{P}\{^1\text{H}\}$ NMR spectrum for samples of this product show 10 resonances in the range δ –110 to –150, with the two dominant peaks centered at δ –138 and –149. There are no resonances detected in the shift range associated with cage species, δ +50 to –20. These data are consistent with intermolecular dehydrohalogenation and subsequent formation of a mixture of low molecular weight oligomers with relatively complex structures.

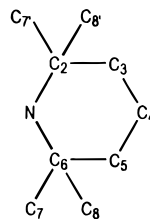
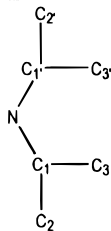
Compound **7**, upon dehydrohalogenation, provides a mixture of a yellow crystalline solid **9** ($\sim 25\text{--}30\%$ by ^{31}P NMR) and a yellow oil **16**. Following recrystallization from hexane, **9** was isolated in 19% yield. The mass spectrum of **9** displays an intense parent ion envelope of ions (m/e 471–463) which is consistent with formation of a cage species $\text{P}_2(\text{Btmp})_2\text{GeMe}_2$. An IR spectrum gives no evidence for a P–H stretching vibration. The $^{11}\text{B}\{^1\text{H}\}$ NMR spectrum and the $^{31}\text{P}\{^1\text{H}\}$ NMR spectrum each contain a singlet centered at δ 48.1 and 42.7, respectively. These compare well with values for the Si analog $\text{P}_2((\text{tmp})\text{B})_2\text{SiMe}_2$: δ 49.2 (^{11}B) and δ 31.3 (^{31}P). The ^1H NMR spectrum of **9** displays three resonances for the tmp group and a singlet for the GeMe_2 methyl protons. The ^{31}P NMR spectrum for the oligomer **16** shows resonances at δ –28 and –79 with no P–H coupling. The mixture also contains a resonance for the known $\text{P}_2(\text{Btmp})_2$, δ –290. Unlike the previously reported cage species, **9** is relatively unstable in solution and the solid state, decomposing $\sim 2\%$ in 30 days to unidentified products.

Dehydrohalogenation of **8** with $^t\text{BuLi}$ gives a pale yellow solid residue which was recrystallized from hexane providing pale yellow crystals, **10**. The compound is isolated in only 44% yield due to its high solubility in both hexane and benzene. The mass spectrum of **10** displays an intense parent ion envelope (m/e 596–587), consistent with the expected molecular weight of the cage compound. The infrared spectrum shows no evidence for P–H stretching vibrations consistent with an intramolecular cage closure reaction of the type already reported for P-borylated⁶ and P-silylated⁷ diphosphadiboretane species. The $^{11}\text{B}\{^1\text{H}\}$ and $^{31}\text{P}\{^1\text{H}\}$ NMR spectra each show a single peak in the shift regions expected for a (tmp)B fragment and

Table 2 NMR Spectral Data for Compounds

	$\delta(^{11}\text{B}\{^1\text{H}\})$	$\delta(^{31}\text{P}\{^1\text{H}\})^a$	$\delta(^1\text{H})^a$	$\delta(^{13}\text{C}\{^1\text{H}\})^a$
1	47.1	-162.8	3.9 (PH) 1.1 (CH ₃)	51.6 (CH) 23.2 (CH ₃) 3.5 (CH)
2	50.8	-127.2	4.7 (PH) 1.52 (tmp)	58.2 (2), 40.9 (3) 33.4 (7), 30.2 (8) 16.5 (4)
3	50.0	-174.9 -91.2	4.1 (PH) 4.12 (CH), 3.78 (CH') 3.39 (DME), 3.2 (DME') 1.45 (CH ₃), 1.38 (CH ₃)	70.7 (DME), 59.4 (DME) 50.6 (CH), 49.3 (CH') 24.8 (CH ₃), 23.5 (CH ₃)
4	53.6	-138.3 -15.5	5.62 (PH) 3.38, 3.13 (DME) 1.93, 1.65 (tmp)	71.8 (DME), 58.8 (DME) 57.0 (2), 44.5 (3) 33.3 (7,8), 17.5 (4)
5	47.1	-146.8 -140.8	4.94 (PH) 4.11 (CH), 3.20 (CH') 1.16 (CH ₃), 1.01 (CH ₃) 0.97 (GeMe ₃)	54.6 (CH), 48.1 (CH') 24.3 (CH ₃), 23.3 (CH ₃) 8.6 (GeMe ₂)
6		-144.3 -134.6		
7	49.0	-111.7 -105.3	5.74 (tmp) 1.65, 1.40, 1.30 (tmp) 1.12 (GeMe ₂)	58.3, 41.7 32.9, 16.3 8.0 (GeMe ₂)
8	49.3	-118.1 -102.1	8.14–8.10, 7.20–7.10 (Ph) 5.8 (PH) 1.47, 1.23 (tmp)	140.9, 134.7 129.8, 128.2 (Ph) 58.3, 41.3 34.1, 32.8 16.2 (tmp)
9	48.1	42.7	1.77, 1.73 1.54 (tmp) 1.15 (GeMe ₂)	
10	47.3	49.8	7.87–7.90, 7.12–7.18 (Ph) 1.68, 1.66 1.50, 1.49 1.48 (tmp)	139.5, 135.7 129.1, 127.6 (Ph) 57.8, 37.8 33.9, 15.2 (tmp)
11	48.7	-142.1 -149.09	5.06 (PH) 4.29, 3.28 (CH) 1.27, 1.16 (CH ₃) 1.08 (GeMe ₂)	54.5, 47.7 (CH) 24.6, 22.5 (CH ₃) 5.7 (GeMe ₂)
12	50.9	-110.9 -100.5		
13	44.3	25.4 14.0	7.90–7.87, 7.20–7.08 (Ph) 1.63–1.28 (tmp)	222.3 (CO _{trans}) 217.2 (CO _{cis}) 136.7, 136.0, 130.0, 128.5 (Ph) 58.0, 35.5, 34.4, 33.2 14.5 (tmp)
14		7.3 6.4	1.58 1.42–1.25 (tmp) 0.81 (GeMe ₂)	222.9 (CO _{trans}) 217.6 (CO _{cis}) 57.9, 36.6, 35.8, 32.2, 14.6 (tmp) 2.25 (GeMe ₂)

^a Coupling constants (Hz): **5**, ¹J_{PH} = 197, ³J_{PH} = 4.0, ³J_{HH} = 6.8 (C₁), ³J_{HH} = 6.8 (C₁'), ³J_{HH} = 6.7 (C₂), ³J_{HH} = 6.7 (C₂'), ³J_{PH} = 1.9 (GeMe₂), ⁴J_{PC} = 1.5 (C₂); **6**, ¹J_{PH} = 199; **7**, ¹J_{PH} = 195, ²J_{PP} = 48, ³J_{PH} = 4.9, ³J_{PH} = 0.9 (GeMe₂); **8**, ¹J_{PH} = 192, ²J_{PP} = 52, ³J_{PH} = 6.3, ²J_{CP} = 12; **11**, ¹J_{PH} = 191, ³J_{HH} = 6.7 (CH), ³J_{HH} = 6.8 (CH), ³J_{HH} = 6.8 (CH₃), ³J_{PH} = 2.5 (GeMe₂); **12**, ¹J_{PH} = 180, ²J_{PP} = 45; **13**, ¹J_{PP} = 44, ²J_{PC_{cis}} = 7.2, ²J_{PC_{trans}} = 3.2; **14**, ²J_{PP} = 57, ³J_{PH} = 2.0 (GeMe₂), ²J_{PC_{cis}} = 7.0



the pyramidal phosphorus atoms in the trigonal bipyramidal cage. The corresponding shifts for P₂((tmp)B)₂SiPh₂ **17** are δ 48.2 (¹¹B) and δ 32.2 (³¹P). The ¹H and ¹³C{¹H} spectra show a single environment for the Ph and tmp rings.

The molecular structure of **10** was determined by single-crystal X-ray diffraction analysis. A view of the molecule is

shown in Figure 1, and selected bond lengths and angles are summarized in Table 3. The molecule has a trigonal bipyramidal structure, similar to that displayed by **17**, with the phosphorus atoms in the apical positions and the (tmp)B and Ph₂Ge fragments in the trigonal plane. The average P–B bond length, 1.973 Å (range 1.983–1.958 Å), is similar to the average

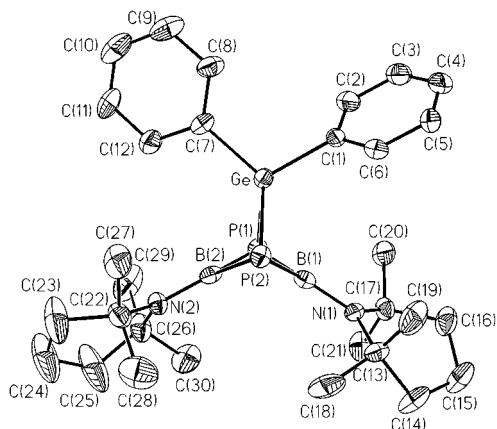


Figure 1. Molecular structure and atom labeling scheme for $P_2(tmpB)_2GePh_2$ (**10**) (30% thermal ellipsoids).

Table 3. Selected Bond Lengths (Å) and Angles (deg) for $P_2(tmpB)_2(GePh_2)$ (**10**), $P_2(tmpB)_2(GePh_2) \cdot Cr(CO)_5$ (**13**), and $P_2(tmpB)_2(GeMe_2) \cdot Cr(CO)_5$ (**14**)

	10	13	14
Bond Lengths			
B(1)–P(1)	1.966(10)	2.020(4)	1.990(5)
B(1)–P(2)	1.985(11)	1.949(4)	2.008(6)
B(2)–P(1)	1.958(12)	1.995(4)	1.965(5)
B(2)–P(2)	1.983(12)	1.980(5)	1.982(5)
Ge–P(1)	2.326(3)	2.331(1)	2.324(1)
Ge–P(2)	2.322(3)	2.310(1)	2.308(1)
Ge–C(1)	1.969(9)	Ge–C(6)	1.944(4)
Ge–C(7)	1.968(10)	Ge–C(12)	1.953(3)
B(1)–N(1)	1.415(13)	1.392(5)	1.389(6)
B(2)–N(2)	1.426(14)	1.391(5)	1.374(7)
Cr–P(1)		2.521(1)	2.503(1)
Cr–C(5)		1.843(4)	1.827(6)
Cr–C(<i>cis</i>) _{av}		1.898(5)	1.889(5)
Bond Angles			
P(1)–Ge–P(2)	80.7(1)	78.9(1)	78.0(1)
Ge–P(1)–B(1)	74.4(3)	77.3(1)	78.5(1)
Ge–P(1)–B(2)	75.1(3)	77.1(1)	76.3(1)
Ge–P(2)–B(1)	74.1(3)	79.2(1)	79.3(1)
Ge–P(2)–B(2)	74.7(4)	77.8(1)	77.1(2)
B(1)–P(1)–B(2)	70.4(5)	69.7(2)	73.0(2)
B(1)–P(2)–B(2)	69.5(4)	71.5(2)	74.0(2)
P(1)–B(1)–P(2)	99.3(5)	96.0(2)	94.9(2)
P(1)–B(2)–P(2)	99.5(5)	95.8(2)	93.8(2)

value in **17**, 1.992 Å, as well as the bond lengths in related cages species $P_2(R_2NB)_2BNR'_2$ ⁶ and $P_2(R_2NB)_2SiR'_2$.⁷ The average P–Ge bond length, 2.324 Å, is, as expected, larger than the average P–Si bond length, 2.243 Å, in **17** due to the larger covalent radius of Ge. The P–Ge distance is slightly longer than the distance in $(H_3Ge)_3P$, 2.308(3) Å,¹⁸ but identical to the distance in the cage species $(Me_2Ge)_6P_4$, 2.322(8) Å.¹⁹ The average P–B–P bond angle in **10**, 99.4°, is similar to the average value in **17**, 98.8°, but the P–Ge–P angle, 80.7(1)°, is slightly smaller than the P–Si–P angle, 84.8(1)°, in **17**. The sums of the internal angles at the phosphorus atoms in **10** are 219.9° (P1) and 218.3° (P2).

The coordination behaviors of **9** and **10** have been examined with equimolar and excess amounts of $Cr(CO)_5 \cdot NMe_3$. In all cases, the 1:1 complexes $P_2((tmp)B)_2(GePh_2) \cdot Cr(CO)_5$ **13** and $P_2((tmp)B)_2(GeMe_2) \cdot Cr(CO)_5$ **14** are obtained as yellow crystalline solids. No evidence is found for coordination of two $Cr(CO)_5$ fragments. Compound **13** provides a weak parent ion envelope in the mass spectrum (m/e 784–781). The infrared

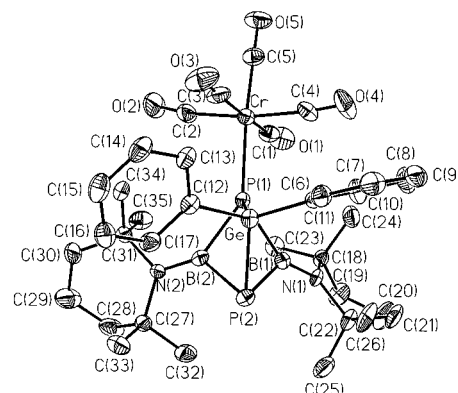


Figure 2. Molecular structure and atom labeling scheme for $P_2(tmpB)_2GePh_2 \cdot Cr(CO)_5$ (**13**) (30% thermal ellipsoids).

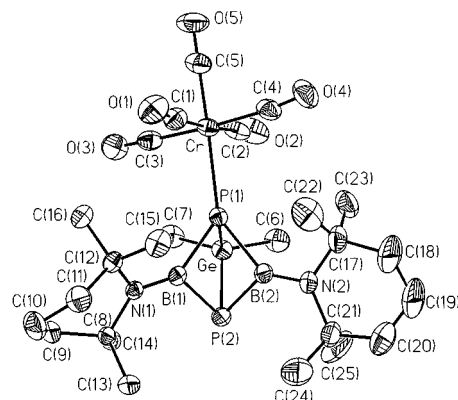


Figure 3. Molecular structure and atom labeling scheme for $P_2(tmpB)_2GeMe_2 \cdot Cr(CO)_5$ (**14**) (30% thermal ellipsoids).

spectra show a characteristic three band pattern in the ν_{CO} region: **13**, 2054, 1985, and 1921 cm^{-1} ; **14**, 2051, 1989, and 1925 cm^{-1} . These values are comparable with the frequencies for $P_2((Pr_2NB)_2((tmp)B) \cdot Cr(CO)_5$:⁶ 2053, 1954, and 1934 cm^{-1} . The $^{11}B\{^1H\}$ NMR spectrum of **13** shows a single resonance at δ 44.3 shifted slightly upfield from the free ligand **10**. The ^{31}P NMR spectra contain two resonances, each split into a doublet by P–P' coupling: **13**, δ 25.4, and 14.0, $^2J_{PP'} = 44$ Hz, and **14**, δ 7.3 and 6.4, $J_{PP'} = 57$ Hz. Each of these is shifted significantly upfield from the resonances of **9** and **10**, and the $^2J_{PP'}$ values are at the upper end of the range so far observed from other $P_2(R_2NB)_2(EX) \cdot (metal\ carbonyl)$ complexes, 45–24 Hz. The lower field doublet has slightly larger line widths, and is assigned to the metal-coordinated phosphorus atom. The $^{13}C\{^1H\}$ NMR spectra show two resonances in the metal carbonyl shift range: **13**, δ 222.3 and 217.2, and **14**, δ 222.9 and 217.6. In each case, the latter is assigned to the *cis* CO due to its relative intensity and larger $^2J_{PC}$ coupling constant: **13**, *cis* 7.2 Hz, *trans* 3.2 Hz, and **14**, *cis* 7.0 Hz, *trans* unresolved. These data are comparable to values reported for $Me_3P \cdot Cr(CO)_5$,²⁰ $Cl_3P \cdot Cr(CO)_5$,²⁰ and $Br_3P \cdot Cr(CO)_5$.²⁰

The molecular structures of **13** and **14** were determined by single-crystal X-ray diffraction analysis and views of the molecules are shown in Figures 2 and 3. In both cases the structure shows a single $Cr(CO)_5$ fragment bonded to one of the apical phosphorus atoms of the cage. The coordinated cage fragment in **13** is compressed slightly along the nonbonding $P \cdots P'$ vector compared to the free ligand: $P \cdots P'$ distances, **13** 2.949 Å, **10** 3.010 Å. The compression is also reflected by the internal cage angles. The angles at P(1) and P(2) are generally larger for **13** relative to **10** and smaller at B(1), B(2) and Ge in

(17) Chen, T.; Duesler, E. N.; Paine, R. T.; Nöth, H. *Phosphorus, Sulfur Silicon* **1994**, 93–94, 73.

(18) Rankin, D. W. H.; Robiette, A. G.; Sheldrick, G. M.; Beagley, B.; Hewitt, T. G. *Inorg. Nucl. Chem.* **1969**, 31, 2351.

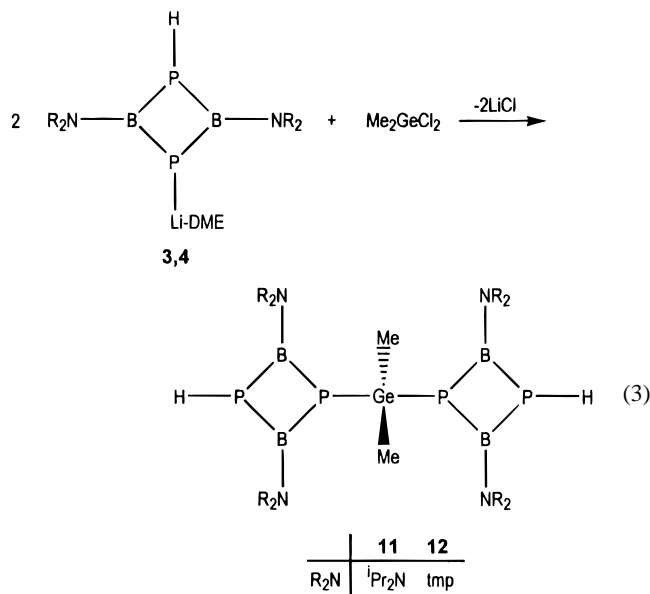
(19) Baudler, M.; Suchomel, H. Z. *Anorg. Allg. Chem.* **1983**, 503, 7.

(20) Davies, M. S.; Pierens, R. K.; Aroney, M. J. *J. Organomet. Chem.* **1993**, 458, 141.

13. Similar trends are observed for **14**. The Cr–P(1) bond lengths, **13** 2.531(1) Å and **14** 2.503(1) Å, are slightly longer than the distances in $P_2(^iPr_2NB)_2((tmp)B) \cdot Cr(CO)_5$ 2.422(1), $Ph_3P \cdot Cr(CO)_5$ 2.486(4) Å²¹ and $((tmp)BPH)_2 \cdot Cr(CO)_5$ 2.458(2) Å.¹¹ The Cr–CO (*trans*) distances, for **13**, 1.843(4) Å, and for **14**, 1.827(6) Å, are significantly shorter than the average Cr–CO (*cis*) distance, for **13**, 1.898(5) Å, and for **14**, 1.889(5) Å, which is consistent with **9** and **10** acting as moderately good σ donors and poor π -accepting ligands. The Cr–CO (*trans*) distances, for example, are shorter than the Cr–CO distance in $Cr(CO)_6$ 1.909(3) Å.²² Similar *trans* Cr–CO bond shortening was observed in $P_2(^iPr_2NB)_2((tmp)B) \cdot Cr(CO)_5$.⁶

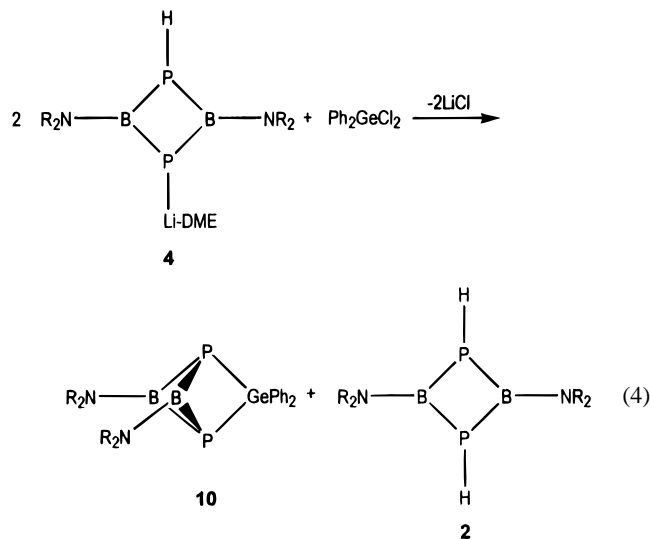
With regard to gaining a greater understanding of the dehydrohalogenation processes, it is noteworthy that combination of **8** with the lithium salt **4** was examined. Two reaction pathways might be anticipated. In one, the lithium salt **4** might act like ^tBuLi initiating dehydrohalogenation of **8** with formation of **10**, LiCl, and the diphosphadiboretane **2**. Alternatively, the phosphide salt might substitute for a chloride on Ge, giving $[(tmp)B)_2P(H)P]_2GePh_2$ and LiCl. In fact, the dehydrohalogenation path is favored, and **10** is formed exclusively over the substitution product. The generality of this reaction has not been tested, although related reactions with *P*-silyl-1,3,2,4-diphosphadiboretanes have been observed.²³ In the present chemical system, the *P*-germyl-1,3,2,4-diphosphadiboretane **7** was combined with $Cr(CO)_5 \cdot NMe_3$ in an effort to prepare a $Cr(CO)_5$ complex of **7**. Instead, a $Cr(CO)_5$ complex, $P_2((tmp)B)_2GeMe_2 \cdot Cr(CO)_5$, **14**, of the cage species **9** was obtained in moderate yield. The mechanism for the formation of **14** has not yet been elucidated, although Me_3N is likely behaving as the base which promotes the dehydrohalogenation of **7**. Whether $Cr(CO)_5$ addition precedes dehydrohalogenation by complexation of a phosphane center in **7** or coordination follows dehydrohalogenation and cage closure remains uncertain.

The 2:1 reactions of **3** and **4** with Me_2GeCl_2 and Ph_2GeCl_2 were also examined and found to give interesting and different results. The 2:1 combination of **3** with Me_2GeCl_2 gives the double chloride substitution product $Me_2Ge[P(^iPr_2NB)_2PH]_2$ **11** as shown in eq 3. Similarly, the 2:1 combination of **4** with



Me_2GeCl_2 gives a double substitution product $Ph_2Ge[P((tmp)B)PH]_2$ **12**. Compound **11** is obtained pure as a yellow solid while **12** typically is contaminated with small amounts of **4** and the cage **9**. The appearance of **9** suggests that dehydrohalogenation of the intermediate **7** competes with the substitution process.

Indeed, the 2:1 combination of **4** with Ph_2GeCl_2 gives the cage molecule **10** and **2** exclusively, and that chemistry is summarized in eq 4.



Neither **11** nor **12** displays a parent ion in the mass spectra, and it is expected that both are susceptible to thermally promoted P–Ge bond cleavage. Both compounds display P–H stretching vibrations in the range 2270–2220 cm^{-1} in infrared spectra. The compounds show a single resonance in the $^{11}B\{^1H\}$ NMR spectra, but two resonances in the $^{31}P\{^1H\}$ NMR spectra. For **11**, the proton coupled ^{31}P NMR spectrum shows a singlet at $\delta -142.1$ and a doublet $\delta -149.09$, $^1J_{PH} = 191$ Hz. Compound **12** gives a similar spectrum with resonances centered at $\delta -100.5$ and -110.9 , but in this case the more downfield member is split into a doublet by P–H coupling, $^1J_{PH} = 180$ Hz, and both resonances are also split into a doublet by P–P coupling, $^2J_{PP} = 45$ Hz.

Conclusion

During our previous studies of the dehydrohalogenation reactions of P-borylated-1,3,2,4-diphosphadiboretanes⁶ and P-silylated-1,3,2,4-diphosphadiboretanes⁷ only intramolecular cage closure products were observed from the chemistry outlined in Scheme 1. In the present study, however, a condition is revealed that appears to favor a competing intermolecular HCl elimination pathway that produces oligomers. That condition is at least large E element (Ge) with small substituents (Me). When the Ge substituent is larger (Ph) with the large amino group tmp present on the B atoms, intramolecular cage closure is favored. More extensive steric influence studies will be required to elucidate all the factors competing in this chemistry, and such work is in progress at this time.

Acknowledgment is made to the National Science Foundation (Grant CHE-9508668) and to the donors of The Petroleum Research Fund, administered by the American Chemical Society, for the support of this research (R.T.P.). A NATO grant initiated the initial collaboration between the research groups in Albuquerque and Munich.

Supporting Information Available: Tables containing details of the X-ray data collection and refinement, heavy atom coordinates, hydrogen atom coordinates, thermal parameters, and complete bond lengths and angles (41 pages). Ordering information is given on any current masthead page.

IC961026N

(21) Plastas, H. J.; Stewart, J. M.; Grim, S. O. *Inorg. Chem.* **1973**, *12*, 265.

(22) Whitaker, A.; Jeffery, J. W. *Acta Crystallogr.* **1967**, *23*, 1977.

(23) Chen, T.; Paine, R. T. Unpublished results.